Supporting Information

CO_2, N_2 and H_2 Adsorption in Zn^{2+}-Containing Zeolites and Metal-Organic Frameworks

Pragnya Paramita Samal[a,b,c], Sailaja Krishnamurty[b,c], Fabian Berger[a,†*], Joachim Sauer[a]

[a] *Humboldt–Universität zu Berlin,* Institute for Chemistry
Unter den Linden 6. 10117 Berlin*, Germany*

[b] *Physical Chemistry division, CSIR–National Chemical Laboratory, Pune 411008, India*

[c] *Academy of Scientific and Innovative Research (AcSIR), Ghaziabad, 201002, India*

† Present address: *Yusuf Hamied Department of Chemistry, University of Cambridge, Cambridge CB2 1EW, UK*

Table of Contents

1. Section S1

1.1 Nomenclature Details of Sites

1.1.1 FAU model

The nomenclature for all sites available in FAU follows the International Zeolite Association (IZA) database.[1] The following site classifications are used:

Site I_a and I_b: Located within the sodalite cage. The two Al atoms are separated by one or two Si units within a six-membered ring (6MR).

Site I_c: Located within two different six-membered rings of the sodalite cage on different planes. The two Al atoms are separated by two Si units.

Site II_a and II_b: Contain two Al atoms distributed with one or two Si units in between within the six-membered ring of the sodalite cage window. These sites point toward the supercage or the exterior.

Site III: Comprises two Al atoms distributed with one Si unit in between within the four-membered ring (4MR) of the sodalite cage window, pointing toward the supercage.

1.1.2 CHA model

Tables S4, S7, and S8 summarise the adsorption properties of the different types of sites available in CHA. In CHA, three distinct ring environments exist: six-membered rings (6MR), eight-membered rings (8MR), and four-membered rings (4MR). Previous studies have shown that Al distributions associated with divalent cation binding in four-membered rings are unstable and experimentally unlikely.[2,3] Accordingly, 4MR sites are not considered further in the present work.

The nomenclature used to describe the remaining sites is as follows. $Zn_{(6MR)}Al_{(6MR-1)}$ and $Zn_{(6MR)}Al_{(6MR-2)}$ denote Zn^{2+} located in a six-membered ring, with the two Al atoms separated by one and two Si units, respectively, within six-membered rings. $Zn_{(8MR)}Al_{(8MR-1)}$ and $Zn_{(8MR)}Al_{(8MR-3)}$ refer to Zn located in eight-membered rings, with the two Al atoms separated by one and three Si units, respectively, within eight-membered rings of CHA. $Zn_{(6MR)}Al_{(8MR-2)}$ denotes Zn located in a six-membered ring, with the two Al atoms separated by two Si units within an eight-membered ring.

For H-CHA, the nomenclature for follows the same convention. $H_{(6MR)}Al_{(6MR-1)}$ and $H_{(6MR)}Al_{(6MR-2)}$ refer to Al distributions with one and two Si units in between within six-membered rings, respectively $H_{(8MR)}Al_{(8MR-1)}$, $H_{(8MR)}Al_{(8MR-2)}$, and $H_{(8MR)}Al_{(8MR-3)}$ refer to Al separations of one, two,

and three Si units, respectively, within eight-membered rings. Similarly, for $Zn(OH)^+$-CHA, $Zn(OH)^+_{(8MR)}Al_{(8MR-1),}$ $Zn(OH)^+_{(8MR)}Al_{(8MR-2),}$ and $Zn(OH)^+_{(8MR)}Al_{(8MR-3)}$ denote Al separations of one, two, and three Si units, respectively, within eight-membered rings.

1.1 Cluster models

For the QM:QM calculations, specific cluster models are employed, as illustrated in Figures 2, 3, S1, and S2. Hydrogen terminations of O atoms with dangling bonds are set to a bond length of 0.953 Å.[4] For FAU, hybrid calculations are carried out on cluster models representing site I and site II, as shown in Figure S1. For CHA, Figure S2 depicts the cluster extracted from the optimized periodic structure for the $Zn_{(6MR)}Al_{(6MR-2)}$ configuration. In this cluster, dangling bonds of Si atoms are saturated with hydrogen atoms at a bond length of 1.455 Å.[4] The cluster model for Zn-MOF-74 includes six Zn cations, five 2-oxidobenzoate anions, one phenolate anion, one formate anion, and six benzene rings, giving a total of 73 atoms. Dangling bonds in this cluster are saturated with hydrogen atoms using two different bond lengths: 1.09 Å for C atoms belonging to the benzene moieties and 0.953 Å for O atoms belonging to the formate and phenolate anions.

2. Section S2

Table S1. Optimized cell parameters of different Zn-based zeolite models studied.

Models	**Si/Al ratio**	**a[Å]**	**b[Å]**	**c[Å]**	**α[°]**	**β[°]**	**γ[°]**
Zn-FAU	23	17.33	17.33	17.39	59.78	60.11	59.98
Zn-CHA	17	13.76	13.76	14.92	90.14	89.97	120.12

Table S2. Relative energies between different Zn^{2+} binding sites (E_{site}) in kJ mol^{-1} for Zn-FAU with a Si/Al ratio of 23, as obtained with PBE+D2 and PBE+D4.

Zn sites	E_{site}	
	PBE+D2	PBE+D4
I_a	5.7	8.9
I_b	54.8	63.9
I_c	116.4	110.2
II_a	0	0
II_b	3.5	4.7
III	134.6	127.9

Table S3. Relative energies between different Li^{+} binding sites (E_{site}) in kJ mol^{-1} for the Li-FAU with a Si/Al ratio of 47, as obtained with PBE+D2 and PBE+D4.

Li sites	E_{site}	
	PBE+D2	PBE+D4
I	0.4	2.3
II	0	0
III	43.6	26.8

Table S4. Relative energies between different Zn^{2+} binding sites (E_{site}) in kJ mol^{-1} for Zn-CHA, with a Si/Al ratio of 17, as obtained with PBE+D4. Also shown are non-scaled stretching frequencies of T–O–T vibrations in cm^{-1}. The frequencies in bold and parentheses are experimental values.[5]

Zn sites	E_{site}	υ_{T-O-T}
	PBE+D4	
$Zn_{(6MR)}Al_{(6MR-1)}$	10	837
$Zn_{(6MR)}Al_{(6MR-2)}$	0	850 **(902)**
$Zn_{(8MR)}Al_{(8MR-1)}$	84	845
$Zn_{(6MR)}Al_{(8MR-2)}$	1	916 **(950)**
$Zn_{(8MR)}Al_{(8MR-3)}$	76	900

Table S5. Calculated adsorption energies (E_{ad}), and enthalpies (H_{ad}) at 298 K for CO_2 and H_2 adsorption in **Zn-FAU** (Si/Al = 23), obtained using PBE+D2. Also reported are zero-point energy corrections (ΔE_{ZPE}), thermal contributions (ΔE_{therm}), entropy contributions ($-T\Delta S_{ad}$), and relative Gibbs free energies (G_{ad}), all in kJ mol^{-1}, at a pressure of 0.1 MPa. The energies in parentheses include high-level corrections using MP2:PBE+D2.

		E_{ad}	ΔE_{therm}	ΔE_{ZPV}	H_{ad}	$-T\Delta S_{ad}$	G_{ad}
CO_2							
	I_a	–54 (–57)	1	6	–47 (–50)	37	–10
	II_a	–48	1	6	–41	42	–1
	III	–79 (–85)	0	6	–73 (–79)	46	–28
H_2							
	I_a	–19 (–12)	–2	5	–16 (–9)	18	3
	II_a	–21	–3	7	–17	24	7
	III	–45 (–40)	–7	10	–42 (–37)	27	15

Table S6. Adsorption energies (E_{ad}), and enthalpies (H_{ad}) at 298 K for CO_2 and H_2 adsorption in **Li-FAU** (Si/Al = 23), obtained using PBE+D2/D4. Also reported are zero-point energy corrections (ΔE_{ZPE}), thermal contributions (ΔE_{therm}), entropy contributions ($-T\Delta S_{ad}$), and relative Gibbs free energies (G_{ad}), all in kJ mol^{-1}, at a pressure of 0.1 MPa.

	PBE+D2					
	E_{ad}	ΔE_{therm}	ΔE_{ZPV}	H_{ad}	$-T\Delta S_{ad}$	G_{ad}
CO_2						
I	–59.4	0.8	6.1	–52.5	42	–10.5
II	–46.5	0.8	6.3	–39.4	37.3	–2.1
III	–55.8	1.4	5.5	–48.9	35.9	–13.0
H_2						
I	–10.5	–10.8	14.6	–6.7	33.2	26.5
II	–23.1	–4	11.2	–15.9	22.9	7.0
III	–28.4	–4.4	11.9	–20.9	24.7	3.8
	PBE+D4					
	E_{ad}	ΔE_{therm}	ΔE_{ZPV}	H_{ad}	$-T\Delta S_{ad}$	G_{ad}
CO_2						
I	–65.7	0.5	6.3	–58.9	42.2	–16.7
II	–45.2	–1.5	6.2	–40.5	45.9	5.4
III	–53.2	1.0	6.5	–45.7	39.6	–6.1
H_2						
I	–7.5	–9.8	13.1	–4.2	34.1	29.9
II	–15.0	–2.3	6.9	–10.4	19.2	8.8
III	–16.3	–2.9	8.1	–11.1	19.6	8.5

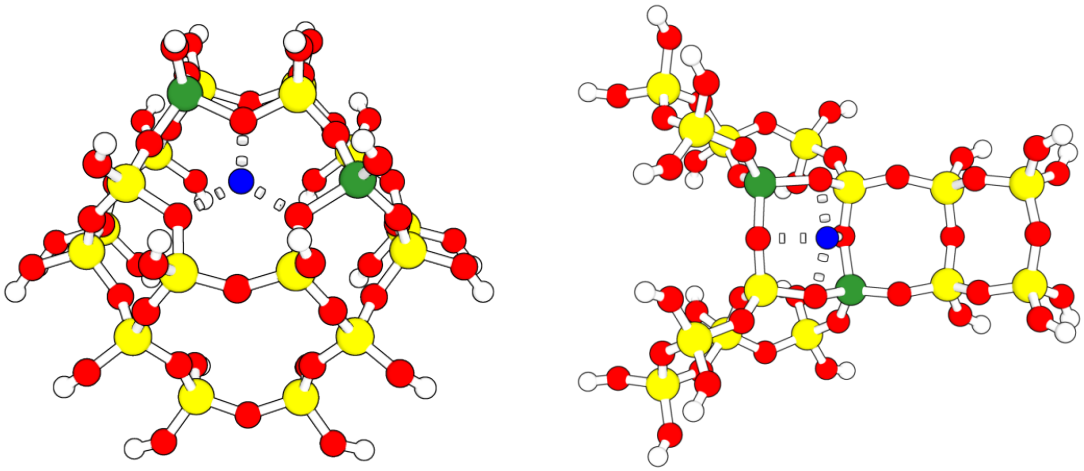

Figure S1. Cluster models as taken from the periodic optimized structure of **Zn-FAU** for MP2:PBE+D2 and MP2:PBE+D4 single-point calculations for site I and site II. Color code: silicon- yellow, aluminum- green, oxygen- red, zinc- blue, and hydrogen- white

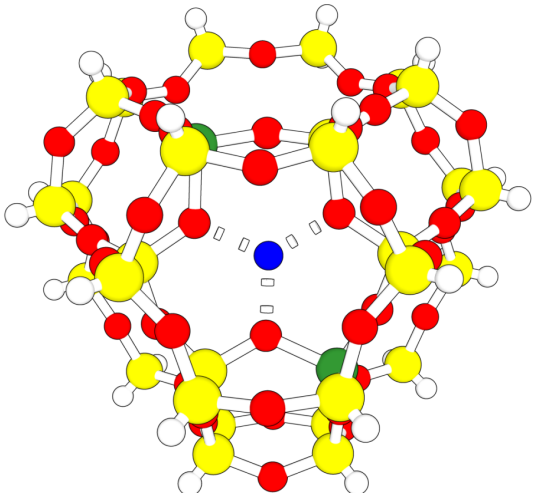

Figure S2. Cluster models from the periodic optimized structure of **Zn-CHA** for MP2:PBE+D4 single-point calculations. Color code: silicon- yellow, aluminum- green, oxygen- red, zinc- blue, and hydrogen- white

Scaling Procedure

The scaling factor *F* is determined following ref. 6. The original approach was subsequently adapted for IR-active vibrations of C=O double bonds.[7] The scaling is introduced to correct for systematic errors arising from both the electronic structure method and the harmonic approximation used to compute vibrational frequencies. Specifically, the scaling factor is defined as the ratio between the experimentally observed asymmetric stretching frequency of gas-phase CO_2, $\upsilon_{CO2,as}^{exp} = 2350\ cm^{-1}$,[8] and the corresponding harmonic frequency calculated at the PBE+D4 level, $\upsilon_{CO2,as}^{comp}$. By applying this factor to CO_2 adsorbed in the materials, the calculated vibrational frequencies are corrected under the assumption that these systematic errors are similar for the same vibrational mode of the same type of bond. This procedure therefore improves agreement with experimental observations without fitting the frequencies to the specific adsorption environment.

$$F = \frac{\upsilon_{CO2,as}^{exp}}{\upsilon_{CO2,as}^{comp}}$$

Table S7. Relative energies between different $Zn(OH)^+$ binding sites (E_{site}), adsorption energies (E_{ad}), and enthalpies (H_{ad}) at 298 K for CO_2 and H_2 adsorption in **$Zn(OH)^+$-CHA** (Si/Al = 17), obtained using PBE+D4. Also reported are zero-point energy corrections (ΔE_{ZPE}), thermal contributions (ΔE_{therm}), entropy contributions ($-T\Delta S_{ad}$), and relative Gibbs free energies (G_{ad}), all in kJ mol^{-1}, at a pressure of 0.1 MPa. PBE+D4 quality wavenumbers for O–H of $Zn(OH)^+$ and adsorbed CO_2 stretching vibrations (υ_{CO2}) in cm^{-1}. The energy in bold includes an experimental value. The scaling factor is calculated as derived according to a procedure explained above, following Sauer et al. [6]

CO_2	E_{site}	E_{ad}	ΔE_{therm}	ΔE_{ZPV}	H_{ad}	$-T\Delta S_{ad}$	G_{ad}	υ_{ZnOH}	υ_{OHsc}	υ_{CO2}
$Zn(OH)^+_{(8MR)}$ $Al_{(8MR-1)}$	30.4	–40.7	–3.1	4.9	–39.1	35.1	–4	3644	3610	2341[a]
$Zn(OH)^+_{(8MR)}$ $Al_{(8MR-2)}$	0	–42.9	–6.0	5.2	–43.7	38.1	–5.6	3675 **3665**	3556	2344[a]
$Zn(OH)^+_{(8MR)}$ $Al_{(8MR-3)}$	9.3	–37.4	–4.4	3.7	–38.1	34.0	–4.1	3648	3638	2346[a]

[a] scaling factor =0.9928, scaling factor for OH frequency = 0.9876

Table S8. Relative energies between different proton binding sites (E_{site}), adsorption energies (E_{ad}), and enthalpies (H_{ad}) at 298 K for CO_2 and H_2 adsorption in **H-CHA** (Si/Al = 17), obtained using PBE+D4. Also reported are zero-point energy corrections (ΔE_{ZPE}), thermal contributions (ΔE_{therm}), entropy contributions ($-T\Delta S_{ad}$), and relative Gibbs free energies (G_{ad}), all in kJ mol^{-1}, at a pressure of 0.1 MPa. Scaled PBE+D4 quality wavenumbers for adsorbed CO_2 stretching vibrations (υ_{CO2}) in cm^{-1}.

CO_2	E_{site}	E_{ad}	ΔE_{therm}	ΔE_{ZPV}	H_{ad}	$-T\Delta S_{ad}$	G_{ad}	υ_{CO2}
$H_{(6MR)}Al_{(6MR-1)}$	0	–43.8	–0.6	6.6	–37.8	41.5	3.7	2348[a]
$H_{(6MR)}Al_{(6MR-2)}$	2.2	–41.5	0.3	6.4	–34.8	36.8	2.0	2350[a]
$H_{(8MR)}Al_{(8MR-1)}$	11.9	–12.2	–0.9	5.6	–7.5	39.6	32.1	2356[a]
$H_{(8MR)}Al_{(8MR-2)}$	1.7	–52.8	–1.4	6.9	–47.3	41.7	–5.6	2354[a]
$H_{(8MR)}Al_{(8MR-3)}$	6.9	–22.9	–1.0	7.6	–16.3	32.8	16.5	2350[a]

[a] scaling factor =0.9928, scaling factor for OH frequency = 0.9876

3. References

(1) Ch. Baerlocher; Darren Brouwer; Bernd Marler and L.B. McCusker. Database of Zeolite Structures; Structure Commission of the International Zeolite Association. 2017.

(2) Paolucci, C.; Parekh, A. A.; Khurana, I.; Di Iorio, J. R.; Li, H.; Albarracin Caballero, J. D.; Shih, A. J.; Anggara, T.; Delgass, W. N.; Miller, J. T.; Ribeiro, F. H.; Gounder, R.; Schneider, W. F. Catalysis in a Cage: Condition-Dependent Speciation and Dynamics of Exchanged Cu Cations in SSZ-13 Zeolites. *J Am Chem Soc* 2016, *138* (18), 6028–6048. https://doi.org/10.1021/jacs.6b02651.

(3) Di Iorio, J. R.; Li, S.; Jones, C. B.; Nimlos, C. T.; Wang, Y.; Kunkes, E.; Vattipalli, V.; Prasad, S.; Moini, A.; Schneider, W. F.; Gounder, R. Cooperative and Competitive Occlusion of Organic and Inorganic Structure-Directing Agents within Chabazite Zeolites Influences Their Aluminum Arrangement. *J Am Chem Soc* 2020, *142* (10), 4807–4819. https://doi.org/10.1021/jacs.9b13817.

(4) Tuma, C.; Sauer, J. Quantum Chemical *Ab Initio* Prediction of Proton Exchange Barriers between CH4 and Different H-Zeolites. *J Chem Phys* 2015, *143* (10). https://doi.org/10.1063/1.4923086.

(5) Fu, D.; Park, Y.; Davis, M. E. Zinc Containing Small-Pore Zeolites for Capture of Low Concentration Carbon Dioxide. *Angewandte Chemie International Edition* 2022, *61* (5). https://doi.org/10.1002/anie.202112916.

(6) Yu, X.; Emmez, E.; Pan, Q.; Yang, B.; Pomp, S.; Kaden, W. E.; Sterrer, M.; Shaikhutdinov, S.; Freund, H.-J.; Goikoetxea, I.; Wlodarczyk, R.; Sauer, J. Electron Stimulated Hydroxylation of a Metal Supported Silicate Film. *Physical Chemistry Chemical Physics* 2016, *18* (5), 3755–3764. https://doi.org/10.1039/C5CP06852E.

(7) Berger, F.; Schumann, J.; Réocreux, R.; Stamatakis, M.; Michaelides, A. Bringing Molecules Together: Synergistic Coadsorption at Dopant Sites of Single Atom Alloys. *J Am Chem Soc* 2024. https://doi.org/10.1021/jacs.4c07621.

(8) Ogren, P. J. Using the Asymmetric Stretch Band of Atmospheric CO2 to Obtain the C=O Bond Length. *J Chem Educ* 2002, *79* (1), 117. https://doi.org/10.1021/ED079P117/SUPPL_FILE/JCE2002P0117W.SIT.